JOURNAL OF PHYSICAL ORGANIC CHEMISTRY
J. Phys. Org. Chem. 2005; **18:** 110–114
DOI: 10.1002/poc.875

Molecular geometry as a source of chemical information. Part 2—An attempt to estimate the H-bond strength: the case of *p*-nitrophenol complexes with bases[†‡]

Tadeusz Marek Krygowski,[1]* Joanna Ewa Zachara[1] and Halina Szatylowicz[2]

[1]Department of Chemistry, Warsaw University, Pasteura 1, 02-093 Warsaw, Poland
[2]Department of Chemistry, Warsaw University of Technology, Noakowskiego 3, 00-664 Warsaw, Poland

Received 27 November 2003; revised 30 March 2004; accepted 16 April 2004

ABSTRACT: B3LYP/6–311+G** optimizations were carried out for *p*-nitrophenol interacting with the flouride with the only constraints for O···F distance in the range 4.0–2.601 Å (for 19 computational data points) with an assumption of planarity of the system and linearity of OH···F. The monotonic dependences of interaction energies on C—O bond lengths led us to propose the C—O bond length as an approximate parameter to measure the H-bond strength. Experimental geometries showed that the C—O bond length is very sensitive, and also that it is the most variable structural parameter in these complexes. Copyright © 2004 John Wiley & Sons, Ltd.

KEYWORDS: H-bond; *p*-nitrophenol; H-bond strength; *ab initio*

INTRODUCTION

Hydrogen bonding is among the most important non-covalent chemical interactions. It appears in a wide range phenomena being a subject of scientific and practical interest.[1–4] On the basis of ISI data (Institute for Scientific Information, Philadelphia (1981–99); retrieved in February 2000) it is known[5] that in the last two decades a paper dealing with H-bonding has statistically been published every half hour! Despite such huge efforts in research, it is not an easy task to estimate the energy of H-bonding. General definition and rules are well known,[2,3,6] but practical applications are accessible mostly to a set of relatively simple cases or, in other words, for a limited number of systems.[3,7] Hence despite the enormous development of theory[3] and computational facilities, there is still a place for empirical approaches.

The energy of the H-bond or, a much more frequently used although less precise term, its strength, is often estimated from some physicochemical properties. Applications of various spectroscopic methods are most often encountered[8] but almost equally often the geometry parameters of H-bond are in use.[7,9–11]

Almost half a century ago, Lippincott and Schroeder[12] introduced a geometry-based potential for OH···O bonds allowing one to estimate their energy. Refinement and extension of this approach to other kinds of H-bonded systems then followed.[13] Simpler geometry-based approaches, based on Pauling's bond number[14] combined with a relation between the bond number and bond energy,[15] led to a fairly effective estimation of the energy of —H···B (base) interactions.[7,16–18] Some speculations on H-bonding strength were based directly on the geometry patterns.[19–21] Geometry-based analysis was one of the most important developments for the concept of resonance-assisted hydrogen bonds (RAHB).[22,23] To our knowledge, apart from the Gilli approach,[22,23] the geometry patterns of more distant parts of a molecule involved in H-bond complexes have not been taken into systematic consideration. The aim of this work was to apply the changes in geometry to estimate the H-bond strength of *p*-nitrophenol–base complexes.

THEORETICAL

The motivation (of the title problem)

In the case of *para*-substituted phenols in which X is an electron-accepting group, the charge transfer from the hydroxyl group to the substituent X is essential as it results from a simple Hammett-like reasoning.[24] The nitro group is strongly electron accepting, particularly when interacting with electron-donating counter substituents. The appropriate substituent constants for the NO_2 group, *para* to OH, $\sigma_p = 0.78$,[25] *para* to O^-, $\sigma_p^- = 1.27$; assuming a strong positive charge on the nitrogen of the NO_2 group in the *para* position, for OH $\sigma_p^+ = -0.92$ and for O^- $\sigma_p^+ = -2.3$.[26]

---

*Correspondence to: T. M. Krygowski, Department of Chemistry, Warsaw University, Pasteura 1, 02-093 Warsaw, Poland.
E-mail: tmkryg@chem.uw.edu.pl

[†]Selected article presented at the Seventh Latin American Conference on Physical Organic Chemistry (CLAFQO-7), 21–26 September 2003, Florianópolis, Brazil.

[‡]Dedicated to our friend and teacher, Professor Andrzej Górski.

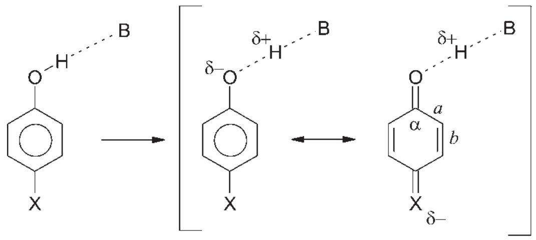

Figure 1. Labelling of geometric parameters and the scheme of the process leading to the intramolecular charge transfer described by the canonical structures on the right

Upon H-bond formation, the electron-donating ability of the hydroxyl group increases, because the process of proton removal from the oxygen atom correlates with an increase in negative charge at the oxygen atom. In consequence, an increase of a quinoid-like structure follows, as shown in Fig 1.

Obviously, the stronger the H-bonding, the more the proton is shifted towards the base, B, and the more negative charge appears on the oxygen atom. In consequence, an increase in quinoid structure weight is observed, caused by the intramolecular charge transfer. This obviously results in changes in geometry: the C—O bond becomes shorter, *a*-bonds become longer and the *ipso* angle α becomes sharper. These parameters are mutually related and this kind of observation was found for a very small set of H-bonded complexes between pentachlorophenol and various bases.[27] It has recently been supported as general relationships for 635 H-bonding complexes of differently substituted phenol derivatives interacting with different bases.[28] The most directly involved and experimentally easily accessible structural parameter of the H-bond donor is the C—O bond length, but two other parameters are also involved in the process of structural changes due to the H-bond formation.

Modelling and computational procedures

Table 1 presents geometric data for 13 *p*-nitrophenol complexes with different bases retrieved from the CSD.[29] It should be mentioned that in almost all these cases, apart from the main interactions being the H-bonding of the hydroxyl group with the bases, there are numerous additional interactions in the crystal lattice. Most often these are the interactions in which oxygen atoms either in the hydroxyl group or in the nitro group are involved in some weak H-bonding with H-donors of the neighbouring molecules. Such interactions clearly obscure the picture of the H-bonding that is the subject of our study.

It is shown that the values of all structural parameters mentioned above vary over a wide range. The most closely related structural parameter involved in H-bonding is the C—O bond length. This parameter varies most, as is seen in the values of variance (Table 1), and therefore it was chosen for further study. To relate these data to the energy of the H-bond, the following simplified model process was set up in which the approach of fluoride along the OH bond direction in *p*-nitrophenol (the constraint) was followed by an optimization procedure (Fig. 2).

The Becke-style three-parameter density functional theory using the Lee–Yang–Parr correlation functional and the 6–311+G** basis set (B3LYP/6–311+G**) were used to optimize the geometries of the molecules and complexes and to calculate vibrational frequencies. Only

Table 1. Geometric parameters (for labelling, see Fig. 1; bond lengths in the ring are taken as the mean values, $\bar{a}$, $\bar{b}$, $\bar{c}$), statistical descriptors of the distributions, CSD[29] reference codes and names of the H-bond complexes of *p*-nitrophenol with different bases (H-donors are in bold face)

Compound name	RefCode	d_{CO} (Å)	$\bar{a}$ (Å)	$\bar{b}$ (Å)	$\bar{a} - \bar{b}$ (Å)	α (°)
4-Nitrophenol 4-methylpyridine[30]	CAXNOE	1.344	1.387	1.375	0.012	119.5
1,4,10,13-Tetraoxa-7,16-diazacyclooctadecane bis(**p-nitrophenyl**) clathrate[31]	GOBYOL	1.345	1.381	1.371	0.010	119.5
4-Nitropyridine *N*-oxide **4-nitrophenol**[32]	JUDNAX	1.347	1.391	1.370	0.021	119.9
Pyridine *N*-oxide **4-nitrophenol**[33]	NILZOX	1.336	1.396	1.370	0.026	119.5
4-Nitrophenol[34]	NITPOL02	1.349	1.404	1.387	0.017	120.2
4-Nitrophenol[34]	NITPOL03	1.359	1.410	1.392	0.018	120.3
2-(*N*,*N*-Diethylamino)methyl-4-nitrophenol **4-nitrophenol**[35]	NUDLON	1.330	1.404	1.381	0.023	119.1
1,5,7-Triazabicyclo[4.4.0]dec-5-ene bis(**4-nitrophenol**)[36]	OFECAD	1.292	1.416	1.371	0.045	117.4
cis, *trans*-Diacetamide **4-nitrophenol** clathrate[37]	VIVYUU	1.351	1.391	1.380	0.011	120.4
N-Butyrylbenzamide **4-nitrophenol** clathrate[37]	VIVZAB	1.355	1.394	1.383	0.011	120.5
2-Picoline *N*-oxide **4-nitrophenol**[38]	WIRWID	1.363	1.381	1.386	−0.005	120.7
2-Pyridone **4-nitrophenol**[39]	OFUGUR	1.348	1.389	1.368	0.021	119.6
Piperazinediium bis(**4-nitrophenolate**) dihydrate[40]	XUTCAQ	1.310	1.409	1.368	0.041	117.1
	Variance	4.0×10^{-4}	1.3×10^{-4}	0.7×10^{-4}	1.7×10^{-4}	1.240
	ESD	0.020	0.011	0.008	0.013	1.1

ESD: estimated standard deviation.

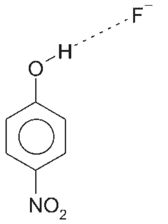

Figure 2. Structural scheme of the computational model. The geometry optimization was carried out for various O···F distances within the range 4.0–2.601 Å

one negative frequency was found, indicating the proper route of proton on the path realized by H-bonding of the system under consideration.

Partial geometry optimization was performed in all cases of complexes of *p*-nitrophenol with fluoride; all the dihedral angles (a planar structure was assumed) and the distance between the oxygen atom in the hydroxyl group and fluoride (for each step within the range 4.0–2.601 Å) were frozen. Moreover, the angle between fluoride and the hydroxyl group was kept equal to 180.0°.

With respect to the calculations of the energies of the molecules and complexes, in order to estimate the *p*-nitrophenol–fluoride interactions, the use of the counterpoise correction method eliminated basis set superposition errors. Two energy terms were calculated: (a) the interaction energy E_{int} between *p*-nitrophenol and fluoride that was calculated according to Eqn (1); (b) the deformation energy E_{def} that is due to the geometry change of the *p*-nitrophenol molecule caused by the interactions with fluoride was calculated according to Eqn (2). All calculations were performed using the Gaussian 98 series of programs.[41]

$$\begin{aligned} E_{\text{int}} = E_{\text{AB}}(basis_{\text{AB}}; opt_{\text{AB}}) - E_{\text{A}}(basis_{\text{AB}}; opt_{\text{AB}}) \\ - E_{\text{B}}(basis_{\text{AB}}; opt_{\text{AB}}) \end{aligned} \quad (1)$$

$$E_{\text{def}} = E_{\text{A}}(basis_{\text{A}}; opt_{\text{AB}}) - E_{\text{A}}(basis_{\text{A}}; opt_{\text{A}}) \quad (2)$$

where A is *p*-nitrophenol and B is F^-. $E_{\text{A}}(basis_{\text{A}}; opt_{\text{AB}})$ means that the energy of molecule A, E_{A}, was calculated using internal coordinates of the A molecule, $basis_{\text{A}}$, and for the geometry obtained during optimization of complex A–B, opt_{AB}. The other terms in Eqns (1) and (2) should be understood in the same way.

The total interaction energy $E_{\text{tot int}}$ was calculated as the difference between the electronic energy of the *p*-nitrophenol–fluoride complex and the energies of *p*-nitrophenol and fluoride.

RESULTS AND DISCUSSION

Following the procedure described above, it was found that the geometry and energy patterns for the full range of O···F distances shows two kinds of interactions. First, the hydroxyl group undergoes a deformation, characterized by elongation of the O—H bond. At an O···F distance of 2.601 Å, the proton transfers to fluoride and the HF molecule is formed. We still have the H-bonding but at this geometry we have another kind of interaction. The HF molecule interacts with the phenolate anion (see Fig. 3). Only the first kind of interaction is the subject of our further consideration. Table 2 presents the data for the above-presented model calculations.

Figures 4 and 5 present the dependence of the interaction energy $E_{\text{tot int}}$ and E_{int}, respectively, on the C—O bond length. In most cases of the experimentally studied H-bonds in *p*-nitrophenol complexes, the base is a neutral molecule. The triangles in Fig. 4 represent the experimental values of C—O bond lengths realized in H-bonding complexes (Table 1). However, some experimental data (for $d_{\text{CO}} > 1.346$ Å) are outside the range of the model curve. These deviations from the model curve are due to the simplified character of the model. However, the nature of interactions is much more complex. In addition to the electrostatic component of the interaction energy, which dominates in our model, in the real system substantial contributions from other forces are also present.

In the case of the dependence presented in Fig. 4, the distribution of the data points follows approximately an exponential curve [see Eqn (3)] based on Pauling's bond number[14] combined with a relation between the bond number and bond energy:[15]

$$E_{\text{tot int}} = D_0\left(\mathrm{e}^{\frac{d_1 - d_{\text{CO}}}{0.37}} - 1\right)^{\frac{1}{c}} \quad (3)$$

where D_0, d_1 and c are −100.876, 1.3479 and 3.7320, respectively, and lead to a correlation coefficient $R = 0.9998$. This analysis follows the ideas presented by Bürgi and Dunitz.[42]

Since the interaction energy described by Eqn (1) does not fit an exponential relationship with the C—O bond length, a polynomial approximation was used.

For stronger H-bonds, the deformation energy [Eqn (2)] increases faster than the interaction energy decreases. Therefore, there is a more complex dependence of the interaction energy on C—O bond lengths, because E_{def} [Eqn (2)] is a component of the total interaction energy

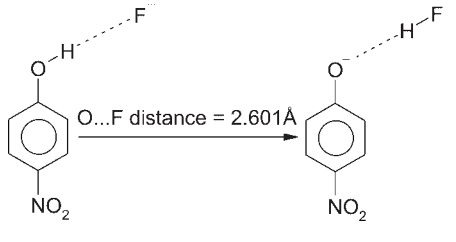

Figure 3. Scheme of the change in the type of H-bond at an O···F distance of 2.601 Å

Table 2. Geometric parameters, energies and statistical descriptors of *p*-nitrophenol complexes with F^- for constrained distances O···F

Fixed O···F distance (Å)	OH distance (Å)	$E_{\mathrm{tot\ int}}$ (kcal mol^{-1})	E_{int} (kcal mol^{-1})	E_{def} (kcal mol^{-1})	d_{CO} (Å)	$\bar{a}$ (Å)	$\bar{b}$ (Å)	$\bar{a}-\bar{b}$ (Å)	α (°)
4.000	0.980	−24.12	−23.66	0.92	1.346	1.406	1.384	0.022	120.4
3.800	0.984	−26.91	−26.74	1.21	1.345	1.406	1.383	0.023	120.4
3.600	0.989	−30.19	−30.41	1.60	1.343	1.407	1.383	0.024	120.4
3.400	0.996	−34.01	−34.73	2.10	1.341	1.408	1.383	0.026	120.4
3.200	1.005	−38.43	−39.61	2.56	1.338	1.409	1.382	0.027	120.3
3.000	1.020	−43.44	−45.31	3.26	1.333	1.411	1.381	0.030	120.0
2.800	1.048	−49.11	−52.75	5.03	1.325	1.414	1.381	0.034	119.5
2.750	1.058	−50.64	−55.12	5.87	1.322	1.415	1.380	0.035	119.3
2.700	1.072	−52.22	−57.98	7.16	1.319	1.417	1.380	0.037	119.1
2.650	1.094	−53.87	−61.78	9.31	1.315	1.418	1.379	0.039	118.8
2.640	1.100	−54.21	−62.78	9.96	1.314	1.419	1.379	0.040	118.8
2.630	1.108	−54.57	−63.94	10.77	1.313	1.419	1.379	0.040	118.7
2.620	1.117	−54.92	−65.32	11.80	1.312	1.420	1.379	0.041	118.6
2.610	1.131	−55.29	−67.31	13.42	1.310	1.421	1.379	0.042	118.5
2.609	1.131	−55.32	−67.37	13.44	1.310	1.421	1.379	0.042	118.5
2.607	1.131	−55.40	−67.49	13.48	1.310	1.421	1.379	0.042	118.5
2.605	1.146	−55.48	−69.30	15.21	1.308	1.421	1.378	0.043	118.4
2.603	1.146	−55.56	−69.43	15.27	1.308	1.421	1.378	0.043	118.4
2.601	1.620	—	—	—	1.271	1.443	1.373	0.070	115.8
Variance	0.004	122.49	250.61	27.03	20.0×10^{-5}	3.0×10^{-5}	0.3×10^{-5}	6.0×10^{-5}	0.7
ESD	0.061	11.07	15.83	5.20	0.014	0.006	0.002	0.008	0.8

($E_{\mathrm{tot\ int}}$). Figure 6 shows this very clearly. It is immediately clear from both the experimental data in Table 1 and computational data in Table 2 that a great variation of structural parameters is observed. It is given by variances, but for easier viewing estimated standard deviations are also given (which are in the same units as the observables). Computational data presented in Figs 4 and 5 clearly show that the changes in d_{CO} may be related to the energy of interactions. This result allows us to suggest C—O bond length changes as a reliable measure of H-bonding strength. Unfortunately, the curves in Figs 4 and 5 cannot be used as the calibration equations, since the modelling presented in this paper refers to the special and very simplified case of the H-bond systems. In our model, the H-bond acceptor is the anion and hence the calculated energies consist of too large a contribution of the electrostatic component of the interaction energy. If the experimental C—O bond lengths are used to estimate the energy of interactions, the values obtained are too high, as shown in Table 3, in the range 20–55 kcal mol^{-1} (1 kcal = 4.184 kJ). These results are much larger than the interaction energy for *p*-nitrophenol with, for example, ammonia (11.03 kcal mol^{-1}), obtained at similar level of theory.[43] This is the most reasonable explanation for why so many experimental C—O bond lengths are situated outside the range of C—O variations estimated by the computational model (Fig. 4). Table 3 presents some estimations from the experimental data.

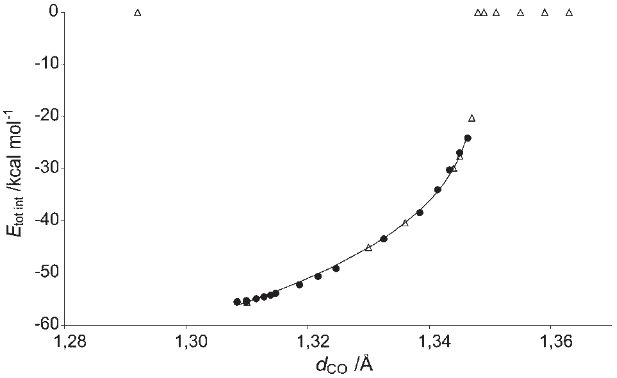

Figure 4. Calculated values of total interaction energy ($E_{\mathrm{tot\ int}}$) as a function of d_{CO} (circles); the triangles represent experimental C—O bond lengths (Table 1). Approximation was made by use of Eqn (3). The data outside the range of the model curve are put on the line of $E_{\mathrm{tot\ ind}} = 0$

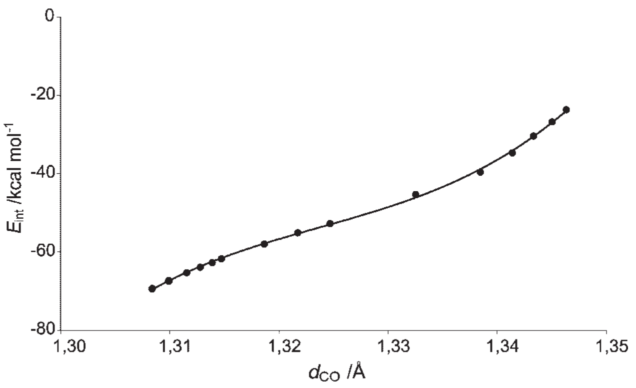

Figure 5. Calculated values of interaction energy [E_{int}, Eqn (1)] as a function of C—O bond lengths (circles) with polynomial approximation curve

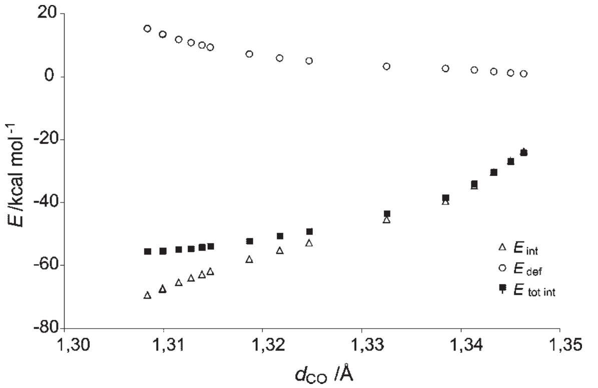

Figure 6. Calculated values of E_{int} [Eqn (1)], E_{def} [Eqn (2)] and the sum of these terms vs C—O bond lengths for the variation of O···F

Table 3. Estimation of the H-bond energy from experimental data when Eqn (3) and polynomial approximations are taken as calibration curves

RefCode	d_{CO} (Å)	E_{def} (kcal mol^{-1})	E_{int} (kcal mol^{-1})	$E_{tot\ int}$ (kcal mol^{-1})
CAXNOE	1.344	1.50	−29.54	−29.88
GOBYOL	1.345	1.23	−27.41	−27.60
JUDNAX	1.347	0.60	−22.73	−20.25
NILZOX	1.336	2.93	−42.57	−40.36
NUDLON	1.330	3.74	−48.94	−45.11
XUTCAQ	1.310	13.39	−67.60	−55.55

Because both dependences of the energy of interactions (E_{int} and $E_{tot\ int}$) on the C—O bond lengths are nicely monotonic, we suggest that the C—O bond length can be used as a qualitative measure of the strength of —OH···B interactions. In this way, easily accessible experimental data may serve for a qualitative estimation of H-bond strength. The general conclusion is that the shorter the C—O bond, the stronger is the OH···B interaction.

Acknowledgements

We wish to acknowledge the Interdisciplinary Centre for Mathematical and Computational Modelling (Warsaw University). We are also grateful to Dr hab. Robert Moszyński for his valuable comments.

REFERENCES

1. Jeffrey GA, Saenger W. *Hydrogen Bonding in Biological Structures*. Springer: Berlin, 1991.
2. Jeffrey GA. *An Introduction to Hydrogen Bonding*. Oxford University Press: Oxford, 1997.
3. Scheiner S. *Hydrogen Bonding. A Theoretical Perspective*. Oxford University Press: Oxford, 1997.
4. Desiraju GR, Steiner T. *The Weak Hydrogen Bonding in Structural Chemistry and Biology.* Oxford University Press: Oxford, 1999.
5. Krygowski TM, Cyrański MK, Czarnocki Z, Häfelinger G, Katritzky AR. *Tetrahedron* 2000; **56**: 1783–1796.
6. Gordon MS, Jensen JH. *Acc. Chem. Res.* 1996; **29**: 536–543.
7. Grabowski SJ. *J. Phys. Org. Chem.* 2004; **17**: 18–31.
8. Sobczyk L. *Ber. Bunsenges. Phys. Chem.* 1998; **102**: 377–383.
9. Legon AC, Millen DJ. *Chem. Soc. Rev.* 1987; **16**: 467–498.
10. Grabowski SJ. *J. Phys. Org. Chem.* 2003; **16**: 797–802.
11. Steiner T. *Angew. Chem. Int. Ed.* 2002; **41**: 48–76.
12. Lippincott ER, Schroeder R. *J. Chem. Phys.* 1955; **23**: 1099–1106.
13. Derrison JD, Smith PH. *Acta Crystallogr., Sect. A* 1978; **34**: 842–853.
14. Pauling L. *J. Am. Chem. Soc.* 1947; **69**: 542–553.
15. Johnston HS, Parr C. *J. Am. Chem. Soc.* 1962; **85**: 2544–2556.
16. Krygowski TM, Kalinowski MK, Turowska-Tyrk I, Hiberty PC, Milart P, Silvestro A, Topsom RD, Daehne S. *Struct. Chem.* 1991; **2**: 71–80.
17. Dziembowska T, Szczodrowska B, Krygowski TM, Grabowski SJ. *J. Phys. Org. Chem.* 1994; **7**: 142–146.
18. Krygowski TM, Grabowski SJ, Anulewicz-Ostrowska R, Izdebski J, Fiertek D. *Pol. J. Chem.* 2002; **76**: 129–135.
19. Ichikawa M. *Acta Crystallogr., Sect. B* 1978; **34**: 2074–2080.
20. Ichikawa M. *J. Mol. Struct.* 2000; **552**: 63–70.
21. Grabowski SJ. *Tetrahedron* 1998; **54**: 10153–10160.
22. Gilli G, Bellucci F, Ferretti V, Bertolasi V. *J. Am. Chem. Soc.* 1989; **111**: 1023–1028.
23. Gilli P, Bertolasi V, Ferretti V, Gilli G. *J. Am. Chem. Soc.* 1994; **116**: 909–915.
24. Hammett LP. *Physical Organic Chemistry.* McGraw-Hill: New York, 1970.
25. Shorter J. *Pure Appl. Chem.* 1994; **66**: 2451–2468.
26. Hansch C, Leo A, Taft WR. *Chem. Rev.* 1991; **91**: 165–195.
27. Woźniak K, Krygowski TM, Kariuki B, Jones W. *J. Mol. Struct.* 1991; **248**: 331–343.
28. Szatylowicz H, Krygowski TM. *Pol. J. Chem.* 2004; **78**: 1719–1731.
29. *The Cambridge Structure Database, version 5.24*, November 2002, updated July 2003.
30. Jin Z-M, Pan Y-J, Xu D-J, Xu Y-Z. *Acta Crystallogr., Sect. C* 2000; **56**: e69–e70.
31. Watson WH, Vögtle F, Müller WM. *J. Inclus. Phenom. Macrocycl. Chem.* 1988; **6**: 491–505.
32. Moreno-Fuquen R, de Almeida Santos RH, Lechat JR. *J. Crystallogr. Spectrosc. Res.* 1992; **22**: 201–204.
33. Moreno-Fuquen R, de Almeida Santos RH, Francisco RHP. *Acta Crystallogr., Sect. C* 1998; **54**: 513–515.
34. Kulkarni GU, Kumaradhas P, Rao CNR. *Chem. Mater.* 1998; **10**: 3498–3505.
35. Filarowki A, Koll A, Głowiak T. *J. Chem. Cryst.* 1997; **27**: 707–719.
36. Ng SW, Naumov P, Chantrapromma S, Raj SSS, Fun HK, Ibrahim AB, Wojciechowski G, Brzezinski B. *J. Mol. Struct.* 2001; **562**: 185–196.
37. Etter MC, Reutzel SM. *J. Am. Chem. Soc.* 1991; **113**: 2586–2598.
38. Moreno-Fuquen R, do Prado Gambardella MT, de Almeida Santos RH. *Acta Crystallogr., Sect. C* 1996; **52**: 1745–1747.
39. Takahashi I, Takahashi M, Morita T, Keumi T, Kitajima H, Wagi M, Hatanaka M, Ohta T, Hosoi S. *Anal. Sci.* 2002; **18**: 619–620.
40. Xiong Y, An T-C, He C, Liu Y, Chen J, Zha CH, Karlsson HT, Chen X. *J. Chem. Cryst.* 2002; **32**: 219–225.
41. Frisch MJ, Trucks GW, Schlegel HB, Scuseria GE, Robb MA, Cheeseman JR, Zakrzewski VG, Montgomery JA Jr, Stratmann RE, Burant JC, Dapprich S, Millam JM, Daniels AD, Kudin KN, Strain MC, Farkas O, Tomasi J, Barone V, Cossi M, Cammi R, Mennucci B, Pomelli C, Adamo C, Clifford S, Ochterski J, Petersson GA, Ayala PY, Cui Q, Morokuma K, Malick DK, Rabuck AD, Raghavachari K, Foresman JB, Cioslowski J, Ortiz JV, Baboul AG, Stefanov BB, Liu G, Liashenko A, Piskorz P, Komaromi I, Gomperts R, Martin RL, Fox DJ, Keith T, Al-Laham MA, Peng CY, Nanayakkara A, Gonzalez C, Challacombe M, Gill PMW, Johnson B, Chen W, Wong MW, Andres JL, Gonzalez C, Head-Gordon M, Replogle ES, Pople JA. *Gaussian 98, Revision A.7.* Gaussian: Pittsburgh, PA, 1998.
42. Bürgi HB, Dunitz JD. *Structure Correlation.* VCH: Weinheim, 1994; vol. 1, Chapt. 1–4 and vol. 2, Chapt. 11.
43. Abkowicz-Bienko AJ, Latajka Z. *J. Phys. Chem.* 2000; **104**: 1004–1008.